Deciphering the non-linear impact of Al on chemical durability of silicate glass

Kamalesh Damodaran, Jean-Marc Delaye, Andrey G. Kalinichev, S. Gin

Deciphering the non-linear impact of Al on chemical durability of silicate glass

Kamalesh Damodaran[a*], Jean-Marc Delaye[a], Andrey G. Kalinichev[b,c], Stephane Gin[a]

a CEA, DES, ISEC, DE2D, University of Montpellier, Marcoule, F-30207 Bagnols sur Cèze, France;

b Laboratoire SUBATECH (UMR6457- Institut Mines-Télécom Atlantique, Université de Nantes, CNRS/IN2P3) Nantes, France.

C National Research University Higher School of Economics, Moscow, Russian Federation.

*** Corresponding author :**

Email - kamalesh.damodaran@cea.fr / kamaleshdams@gmail.com

Phone - +33 752143332

Postal address – Kamalesh Damodaran, DES/ISEC/DE2D/SEVT/LCLT, CEA Marcoule, F-30207 Bagnols sur Cèze, France.

ABSTRACT

The role of Al in aluminosilicate glasses remains somewhat a mystery: at low concentrations, it increases the resistance to hydrolysis of the glass, whereas at high concentrations an opposite effect is observed. To understand the origin of the phenomenon on a fundamental atomistic scale, we performed 577 MD simulations and applied potential mean force (PMF) calculations to estimate the activation barriers for hydrolysis and to statistically correlate them with local structural features of the glass. Models of pure silicate and aluminosilicate glasses are constructed and investigated. PMF simulation results are further validated by the experimental measurements and revealed that Al is very easy to dissociate, but it also increases the glass chemical durability through significantly increasing both the strength of Si and network connectivity of the glass. In contrast, at high Al concentration, preferential dissolution of Al weakens the silicate network, which it supposes to strengthen, and so the glass resistance becomes poor. Through PMF calculations, we evaluated the activation barriers for dissociating bonds around Al as 0.49 eV, which is less than a half of the energy to dissociate bonds around Si in pure silicate (1.22 eV) and around Si in aluminosilicate glass (1.34 eV), all these energy differences being statistically significant. Molecular structural level investigation revealed that Si with Al as a second neighbour in the glass network has a significantly higher activation energy for dissociation than Si in pure silicate glass. The proposed approach opens the way to the development of quantitative predictive models of glass durability.

Keywords: Molecular dynamics simulation; Glass water resistance; Non-metallic glasses; Metallic glasses; Statistics;

1. INTRODUCTION

Crystalline and amorphous silicates are the most abundant natural materials in the Earth's crust[1,2] and also constitute an important component of many man-made materials, such as glasses, ceramics, cements, etc. The ability to quantitatively assess their behaviour over the geological timescale is critical to address many fundamental concerns, including the safe and secure storage of nuclear waste in the form of glass under the conditions of a geological repository[1,3,4], the understanding of weathering processes controlling the mass balance of the ocean[5], and geological CO_2 sequestration[6].

Aluminoborosilicate glasses are used for the immobilization of radionuclides and minor actinides arising from the spent nuclear fuel reprocessing. These glasses are supposed to be stored in a deep geological repository as the most accepted technology for nuclear waste disposal and storage by many countries[7,8]. However, the safety assessment of the storage can be strongly affected by irreversible transformation of these glasses because of their contact with water on a geological timescale[7,9,10]. The best way to evaluate the long-term glass performance is by developing good quantitative understanding of the preponderant mechanisms of glass-water interaction and by deriving a predictive model based on these mechanisms that would allow a reliable extrapolation on very long timescales the potential release of radionuclides into the geosphere from the nuclear waste packages. Due to such a great interest, the dissolution mechanisms of these glasses have been thoroughly investigated for decades through experimental and computational approaches[3,11–19]. However, some fundamental questions regarding glass compositional effects on its chemical durability still remain unsolved[18–21]. It must be kept in mind that chemical durability is a general term that covers many aspects, including ion-exchange, matrix dissolution, passivation by surface layers, precipitation of secondary phases, etc. Here, we focus on the glass behaviour far from saturation, i.e. in conditions where glass undergoes only hydrolysis reactions, which corresponds to the most detrimental effect for the material.

It is reported in the literature that the addition of Al_2O_3 into silicate glass improves its mechanical properties, chemical durability and optical properties[22–25]. Similarly, the addition of Al into the borosilicate glass significantly decreases the dissolution rate of glass elements in water[9]. Hamilton and al. have investigated the effect of the Al/Si ratio on the plagioclase glass dissolution from pH 1 to pH 12[26]. They observed that the dissolution rate of three glasses is increasing with increasing the Al/Si ratio independent of the pH, which is contradictory to the case of nuclear waste glass where the addition of Al significantly lowers the dissolution rate[26]. It is observed experimentally that the addition of Al in small quantities to a silicate glass leads to a strong decrease in the dissolution rate whereas the addition of Al in glass at very high concentrations significantly increases the dissolution rate[27]. However, the fundamental mechanisms regulating this controversial role of Al are hardly accessible through experimental approaches and poorly understood in the glass community even through atomistic computer simulations.

In previous studies, molecular dynamics (MD) simulation method has been widely used to model the glass structure depending on its composition and several approaches have been used to investigate the activation barrier for dissociating the bonds around Si by water[11,28–30]. However, no correlations of the activation barriers with the structural features of the glass are yet available in literature, while this is the key to understand the fundamental role of Al in glasses. Experimental studies estimated the activation energy for dissolution of Si to be within the range of 14-24 kcal/mol[31–33]. Ab initio calculations for small silicate clusters indicate the activation energy to be in range of 18-39 kcal/mol[28–30]. Another ab initio study[34] has demonstrated that Al dissolves preferentially to Si in aluminosilicate glass, which complicates the understanding of mechanisms by which Al increases the durability of glass against water[9]. Recent MD simulations using the potential of mean force (PMF) approach were conducted only for pure silicate glass and observed that the rate-limiting step for dissolution of the bond around Si is due to Si with three or two bridging oxygen atoms[11]. The scale of the activation energy for these two local structural

environments is very small with large standard deviation, making it very difficult to find the actual rate-limiting step controlling the durability of the glass.

For these reasons, we are proposing here a comparative study between the pure silicate and an aluminosilicate glass to estimate the activation barrier for dissociating the bonds around Si and Al by statistically averaging over a large number of local structural situations to address the following four open questions:

1) What is the rate-limiting step for dissociating the bonds around the Si and Al atoms in silicate and aluminosilicate glasses?

2) What are the structural features of the glass contributing towards the durability in both pure silicate and aluminosilicate glass?

3) Does the addition of alumina to pure silicate glass yield a significant rise in durability due to a synergistic effect of Si and Al or due to the individual contribution of Al?

4) What mechanism can explain the higher durability of aluminosilicate glass over pure silicate glass?

Two mechanisms were proposed previously to explain this phenomenon. Firstly, the addition of alumina reduces the sodium ions bonded to non-bridging oxygen atoms (easy to leach) by consuming them as a charge compensator for the tetrahedral co-ordination $[AlO^4]^-$ (comparatively harder to leach). Secondly, the addition of Al_2O_3 would increase the network connectivity of the glass that resists the diffusion of water[13]. We address the four questions above by developing an automated pipeline of MD simulations which takes the glass composition as an input, then creates a glass model, adds water molecules onto its surface, relaxes the system, performs PMF calculations between an H_2O molecule and a target glass forming atom, finally stores all the structural information of the target atom (like the coordination environment, bond angles, local hydrostatic pressure and shear stress force) together with their corresponding activation energy. This method of analysis allows us to statistically decipher the role of Al towards the increased durability of aluminosilicate glass. Agreement of these simulation results with available experimental data

strengthens the reliability of our answers and the method used. As a whole, we demonstrate the mechanism by which Al atoms play two different roles based on their concentration in aluminosilicate glass.

2. MATERIALS AND METHODS

2.1 Glass models preparation

Silicate and alumino-silicate glasses were modelled using the MD simulation approach with the DL_POLY software package[35]. For preparing the silicate glass model structure, 130 Si atoms and 260 O atoms were randomly placed into a cubic simulation box initially with the side of 18.06 Å. For preparing the aluminosilicate glass model, the simulation box contained 38 atoms of Al, 25 atoms of Ca, 252 atoms of O, and 85 atoms of Si. The positions of all atoms in the simulation box were initially relaxed for 10,000 MD steps (1 time step = 1 femtosecond) at a temperature of 1000 K. The interatomic interactions in the system were described by the Mahadevan[36] potential with a 8 Å cut-off radius for short-range non-electrostatic interactions while the long-range Coulombic interactions were treated by the Wolf summation method[37]. The reason why we have preferred to use this potential instead of another one, for example ReaxFF, is developed in the discussion.

The glass model preparation for each system then continued in several stages. The system was equilibrated at a temperature of 4000 K for 100,000 time steps in the *NVT* statistical ensemble (constant number of particles, constant volume, and constant temperature). Subsequently, a thermal quench was applied by decreasing the temperature of the systems in multiple 100 K decrements until the target 300 K temperature was reached. At each intermediate temperature, the system was equilibrated in the *NVT* ensemble for 20,000 steps. The equilibrium volume of the system at 300 K was then determined in a further *NPT*-ensemble MD simulation (constant number of particles, constant pressure, and constant temperature) for 20,000 steps at a pressure of 1 bar. Finally, the systems were further relaxed for 5,000 time steps in the *NVE*-ensemble MD simulation (constant number of particles, constant volume, and constant energy) using the equilibrium state determined

previously to obtain the modelled structure of glass. The glass preparation procedure followed in this study is discussed in more details in a previous work[38].

2.2 Addition of water on the glass surface

The size of the simulation box containing prepared bulk glass models was then doubled along the *z*-axis to create an empty space for the addition of water molecules to form a water – glass interface. The simulation BoxA (containing the glass and the empty space) was then relaxed through a *NVT*-ensemble MD run for 10,000 steps at 10 K to control the mobility of atoms and allow the stabilisation of the surface. Subsequently, an additional relaxation in the *NVT* ensemble for 10^6 steps at 300 K was applied to BoxA. Then a final relaxation was performed in the *NVE* ensemble at 300 K for 5,000 steps.

In parallel, an empty simulation box of exactly the same size was prepared into which H_2O molecules were added randomly to equilibrate bulk liquid water with a density of 1 g/cm^3 (BoxB). The water box was equilibrated under the *NVT* (100,000 steps) and *NVE* (100,000 steps) ensemble at 300 K using the SPC/E water potential[39]. To create the glass – water interface we superimposed the two boxes BoxA and BoxB. A 0.6 Å cut-off distance was applied so that the H_2O molecules whose one atom is less than 0.6 Å from one atom of the glass are eliminated. After this operation, we observe that a few water molecules are still present inside the rings of the glass structure. Those water molecules have been removed manually.

Dissociative potentials[36] were used to relax the (glass + water) system in the *NVT* ensemble at 10 K for 100,000 steps, then at 300 K for 10^6 steps, and finally in the *NVE* ensemble at 300 K for 50,000 steps, to allow the equilibration between the bulk water and the glass surface. A pipeline in *python* was developed to automate the process of glass model preparation until the glass-water interface creation, and was used to prepare 17 independent models of pure silicate glasses and 25 independent models of aluminosilicate glasses to improve the statistics of the PMF calculations. This pipeline is presented graphically in Figure 1.

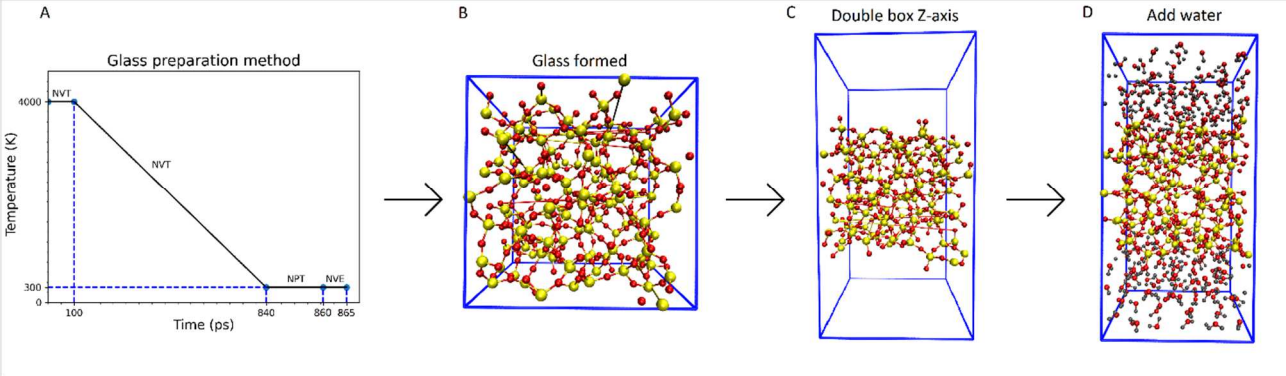

Figure 1. Graphical flowchart of the glass model preparation for further PMF calculations. A) Glass preparation procedure through classical MD simulation method. B) Snapshot of the prepared glass as per protocol in (A). C) Snapshot of the box size doubled along the *z*-axis. D) Addition of water into the empty space of the simulation box. Color scheme: Yellow – Si glass forming element; red – oxygen atoms; gray – hydrogen atoms.

2.3 PMF calculations

Potential mean force (PMF) calculations were used to quantitatively estimate the activation barrier required for the hydrolysis of the Si-O-Si bonds in pure silicate glass and Si-O-X or Al-O-X bonds in aluminosilicate glass (The second neighbouring atoms of the aluminosilicate glasses are represented as X throughout the study because they can be either Al or Si). To apply the PMF method, one water molecule was progressively moved closer to one atom of the glass surface (the target atom) by gradually imposing a lower and lower distance between the two. A complete PMF calculation requires a number of separate MD simulations to cover all the possible distance between water molecule and the glass atom (the reaction coordinate). In each of these "sampling windows" the distance between the reacting species is restrained at a particular position using a harmonic force to allow the system to sample all possible configurations around that particular value of the reaction coordinate. The additional force required for maintaining each intermediate distance is registered and the integration of this force along the reaction coordinate followed by the water molecule corresponds to the free energy required to approach the water molecule near the target atom[11].

To have a large statistics for the PMF calculations, we have performed them for all the water molecules located close to the Si or Al atoms of the glass within a cut-off radius of 3.5 Å. When several water molecules are within the cut-off radius around one target atom, the closest water molecule to this target atom was selected. The distance constraints were applied between the O atom of the water molecule and Si or Al atoms of the glass by gradually decreasing the distance between them by steps of 0.05Å until the constraint distance reached 1.5 Å. For each intermediate distance, the system was relaxed during 10,000 time steps in the *NVT* ensemble. The average additional force applied to maintain the separation distance was calculated during the last 9,000 time steps at each distance. The integration of the complete profile of the additional force plotted against the constraint distance between the two atoms yields the activation barrier. The method was applied to estimate the activation energies necessary to dissociate the Si-O-Si, Si-O-Al, Al-O-Si and Al-O-Al bonds in pure silica and in the aluminosilicate glasses. (The atom before the oxygen in this notation represents the target atom of the PMF calculation, the atom after the oxygen represents the second neighbour, and the bond is broken between the target atom and the oxygen). In some PMF calculations, water molecules did not dissociate any of the above-mentioned bridges; those activation energies were discarded to construct the clean dataset of bond dissociation energy against their structural features. To correlate these activation energies with structural features, we also calculated the bond angle, local hydrostatic pressure and shear stress force of the atoms, correspondingly. Local shear stress on one atom was calculated with the following equation:

$$\sigma_{ij}^{m} = -\frac{1}{V_m}\left[\frac{1}{2}\sum_{n=1,n\neq m}^{N} x_i^{mn} f_j^{mn} + m^m v_i^m v_j^m\right] , \qquad (1)$$

where x_i^m and v_i^m are the position and velocity of the atom m along the i direction, f_i^{mn} is the force exerted by the atom n on the atom m in the i direction. The summation is done over all the neighbouring atoms around one particular atom using a cutoff radius of 8 Å. V_m corresponds to the local volume around the atom m. Here the average volume per atom (V_{total}/N) is used.

Hydrostatic pressure were derived from the local shear stress tensor as follows:

$$p(i) = \frac{\left(\sigma_{11}^{i} + \sigma_{22}^{i} + \sigma_{33}^{i}\right)}{3} \ , \tag{2}$$

$$\tau(i) = \sqrt{3p(i)^2 - \Sigma(i)} \ , \tag{3}$$

where $\Sigma(i) = \left(\sigma_{11}^{i}\sigma_{22}^{i} - \sigma_{12}^{i}\sigma_{21}^{i}\right) + \left(\sigma_{22}^{i}\sigma_{33}^{i} - \sigma_{23}^{i}\sigma_{32}^{i}\right) + \left(\sigma_{11}^{i}\sigma_{33}^{i} - \sigma_{13}^{i}\sigma_{31}^{i}\right)$. These local hydrostatic pressure and shear stress forces exerted on the target atom are calculated[40,41] to correlate with their activation energy.

2.4 Statistical tests to investigate the hypothesis

The quantitative data generated during these simulations were subjected to different statistical tests to investigate if the mean of two groups under the comparison are significantly different or not. To investigate if the distribution of data is normal or not, the Kolmogorov-Smirnov test was used when the size of the sample was more than 50 and the Shapiro-Wilk test was used when the size of the sample was less than 50[42,43]. The distribution of data is considered normal for the P-values greater than 0.05, whereas it is not normal when the P-values are less than 0.05[42]. Non-parametric tests were selected if the distribution of the two groups under the comparison is not normal, whereas parametric tests were used for the normally distributed data[44]. For comparing the two groups of data with unequal sample sizes, we applied the Welch's t-test for the parametric tests and the Mann-Whitney U-test for the non-parametric tests. In both cases, the P-values less than 0.05 mean that the two sets of data under comparison are significantly different, whereas if the P-values larger than 0.05 indicate that the difference between the means of the two data sets is not statistically significant.

2.5 Leaching experiments of ISG-AL-05 and ISG-AL-06 in distilled water

Leaching experiments were performed with the ISG-AL-05 (40.6 SiO_2, 16.8 Al_2O_3, 16.5 B_2O_3, 4.8 CaO, 18.3 Na_2O, 3.1 ZrO_2 in mass %) and ISG-AL-06 (26.4 SiO_2, 26.5 Al_2O_3, 15.7 B_2O_3, 4.5 CaO, 23.8 Na_2O, 3 ZrO_2 in mass %) glass powders with particle size range of 75 – 150 μm. These two glasses belong to a series of glasses already studied numerically and experimentally [45,46]. The specific surface area, measured by the Brunauer, Emmett and Teller (BET) method was

equal to 220 cm^2/g and 210 cm^2/g, respectively, and the leaching solution was 18 MΩ.cm deionized water initially adjusted and maintained during the experiment at $pH^{90°C}$ 7. Small quantity of lithium chloride was added to help the probe sense and optimize the pH of the distilled water.

Then 0.1072 g of ISG-AL-05 and 0.0430 g of ISG-AL-06 was added to the 250 ml and 400 ml of the solution respectively, to investigate the initial dissolution rate of these two glasses. Samples were taken from the solution containing the ISG-AL-06 powder every 45 minutes during the 4 hours of the experiment and from the solution containing the ISG-AL-05 powder at every hour during the 7 hours of the experiment. Then the samples were analysed by inductively coupled plasma-optical emission spectrometry (ICP-OES at FiLAB – Laboratoire d'analyses en chimie organique, minéraux et matériaux in France) with ±5% uncertainties to estimate the concentration of Si, B, Al and Na released from the glass powders. From the concentration data, the normalised mass loss was calculated as follows:

$$NL(i)(g \cdot m^{-2}) = \frac{C(i) \cdot V}{S \cdot x_i} + \sum NL(i)_{samplings} \quad (4)$$

where $C(i)$ is the concentration of an element i in the solution, V is the solution volume, S is the glass surface area, x_i is the mass fraction of i in the glass, and $\sum NL(i)_{samplings}$ represents the contribution of the various samples taken in the leachate.

The initial dissolution rates of the two glasses, r_0, were calculated from linear regression of the normalized mass loss of Si. To capture the dissolution of the first few nanometers of the polished glass coupons of ISG-AL-05 and ISG-AL-06, both were leached in distilled water with neutral pH at 90°C for 1 hour and 5 minutes, respectively. The altered glass surfaces were analysed by X-ray photoelectron spectroscopy (XPS) and by time-of-flight secondary ion mass spectrometry (ToF-SIMS). XPS (NOVA – KRATOS, TESCAN ANALYTICS, France) was used to quantitatively estimate the elemental composition of the glass surface before and after leaching for both the coupons. The analysis was conducted with a 75 W Al Kα beam, with charge compensation and a 0° detection angle. The analysed surface was 300×700 μm^2 and the depth of analysis was < 10 nm. The uncertainty on the Al/Si ratio was estimated to be around 10%. ToF-SIMS (IONTOF GmbH

TOF 5 spectrometer, TESCAN ANALYTICS, France) was used to perform a semi-quantitative depth-profiling analysis of the altered ISG-AL-05 sample. The analysis was performed under the following conditions: primary beam of Bi_1^+ 25 KeV ~ 1.7 pA and O_2^+ 1 KeV, 306 nA to record positive ions in the analysis area of 60×60 μm² and 190×190 μm², respectively. More detailed information about the application of ToF-SIMS to glass analysis can be found elsewhere[47].

3. RESULTS

3.1 Time step optimization to perform PMF calculations and to estimate the activation barrier

To determine the activation barriers corresponding to the dissociation of the bonds in the silicate and aluminosilicate glasses using PMF calculations, we first performed a small pilot study to estimate the number of steps required to obtain stabilized values. The numbers of steps selected to test the PMF method were 1000, 3000, 5000, 8000, 10000 and 15000. The PMF calculations were performed using one glass containing 23 Si atoms that are in close contact with H_2O. The distribution of the activation energies are shown in Figure 2.

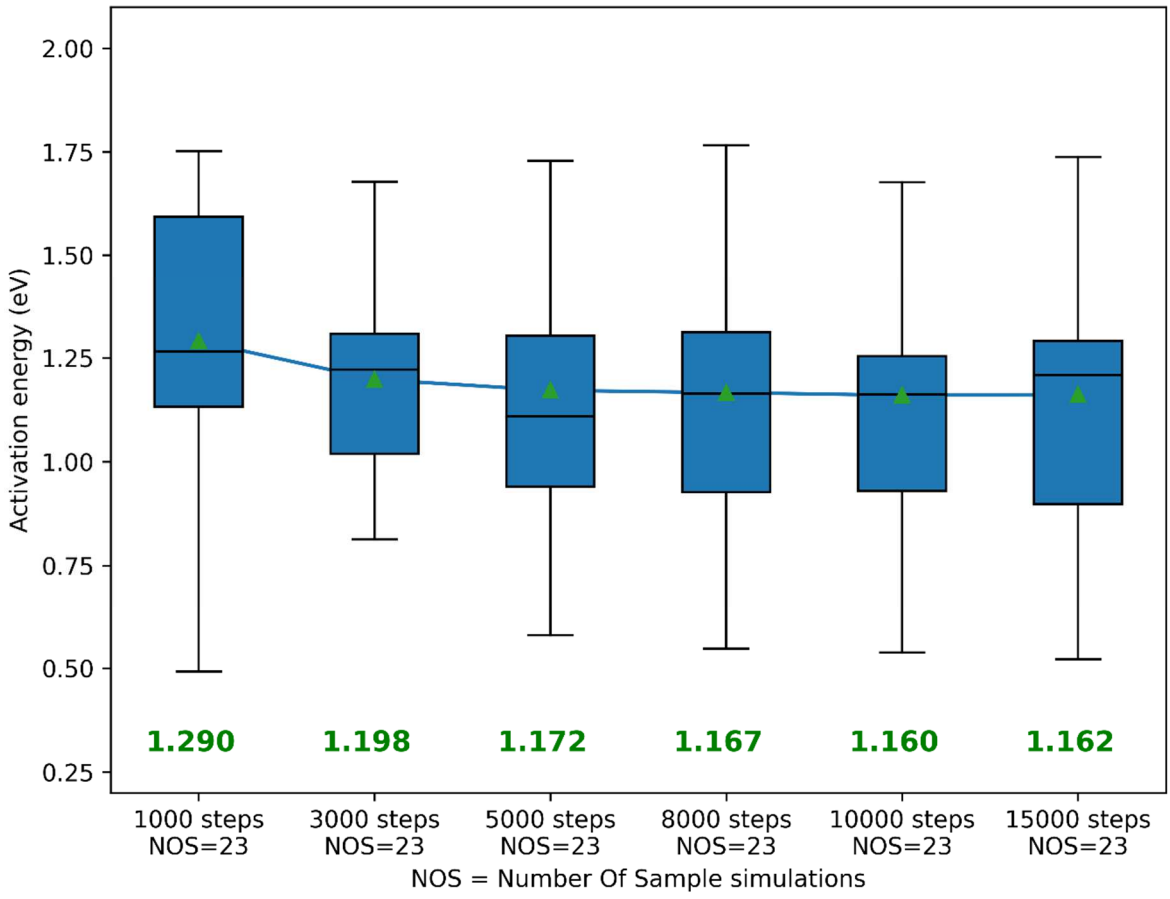

Figure 2. Activation energy distribution for bond dissociation of Si in pure silicate glass with different number of optimization steps. The green triangles represent the mean values; the blue line connects the mean; the exact mean value is displayed in green colour below each boxplot, respectively; the boxplot represent the standard Q1 – 25th percentile, Q3 – 75th percentile and median – 50th percentile. The two whiskers extending the boxplot represent standard boxplot minimum and maximum.

For 1000 steps duration, relaxation of the glass structure is not yet sufficient, leading to a significant overestimation of the activation energy. With increasing the number of steps, the average activation barrier decreases and starts to stabilize beyond 5000 steps. The mean activation energies for the last three durations are converged within the range of 1.16 to 1.167, as shown in Figure 2. Thus, we chose to apply the PMF calculations with a duration equal to 10,000 time steps for the relaxation at each intermediate distance.

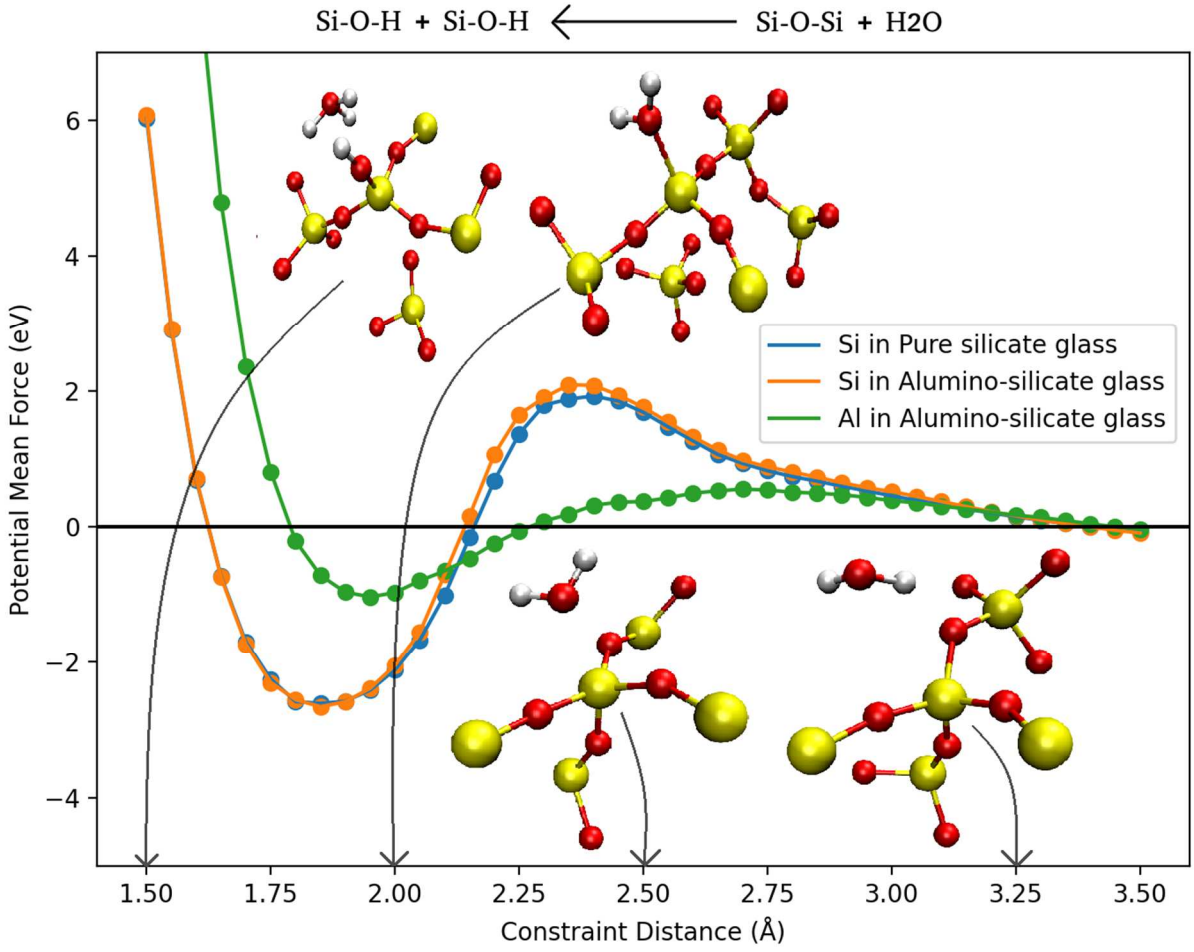

Figure 3. Average activation barrier for dissociating Si in pure silicate, Si and Al in aluminosilicate glass. Blue – bond dissociation around Si in pure silicate glass; orange – bond dissociation around Si in aluminosilicate glass; green – bond dissociation around Al in aluminosilicate glass. The H_2O molecules approaching towards the Si–O–Si bridge is visualized at each step and the constraint distance of the snapshots are pointed by the arrows.

With the PMF method, we estimated the activation barriers of chemical reactions corresponding to the water molecule dissociating the bonds around the glass network formers[48] as shown in Figure 3. Quantitatively investigating this chemical reaction is crucial for assessing the durability of the glass because bond dissociation offers the way for water molecules to diffuse through the glass[9,21,49]. In both pure silicate and aluminosilicate glasses, water molecule approaching towards the target glass network former atom, establishes an additional bond between the oxygen of H_2O and Si or Al atom of the glass around 2.35 Å during the intermediate stage of the

calculation. Subsequently, moving H_2O more towards the Si-O-Si, Si-O-Al, Al-O-Si or Al-O-Al surface bridge, it undergoes dissociation[11].

3.2 Estimating activation barrier for the bond dissociation

For the statistical analysis of the activation energies for water dissociating the Si–O–Si bridges in pure silica, and the Si–O–X and Al–O–X bridges in aluminosilicate glass, we performed PMF calculations for all the 17 models of pure silicate and 25 models of aluminosilicate glasses. Using 3.5 Å as the cut-off radius for the pure silicate glass models, 282 calculations have been performed approaching water molecules close to the Si–O–Si bridges. Similarly, for the aluminosilicate glass models, 227 and 68 calculations have been performed approaching the water molecules close to the Si–O–X bridges and Al–O–X bridges, respectively. The distance between the water molecule and the target atom has been restrained and progressively decreased to estimate the bond dissociation energy of the three bridges by water.

As shown in Figure 4, the mean activation energy of 1.34 eV for dissociating bonds around the Si in aluminosilicate is comparatively higher than for Si in pure silicate with the mean of 1.22 eV. The mean activation energy required to dissociate Al atom in aluminosilicate glass is equal to 0.49 eV, which is not even half of the activation energy for dissociating Si. Such a low activation energy is quite surprising, because the addition of Al atom into a silicate glass is expected to improve the mechanical properties and chemical durability of the glass[1,50].

To investigate if these differences in the activation energies are significant or not, we have first analysed the distribution of data using the Kolmogorov-Smirnov test whose P-value is given in the Table A1 (see the Appendices). Based on the P-values, the bond dissociation energies of Si in pure silicate and Si, Al in aluminosilicate are not normally distributed. Since the sample sizes are not equal and their distributions are not normal, we chose the non-parametric Mann-Whitney U-test (MWU) to investigate if the means are significantly different or not. The P-values < 0.05 indicate that the means of the two compared sets of data are significantly different. In Figure 4, by keeping Si in pure silicate as a reference, we performed the MWU test for other two sets of data and found

that the mean dissociation energies of both Si and Al in the aluminosilicate glass are significantly different.

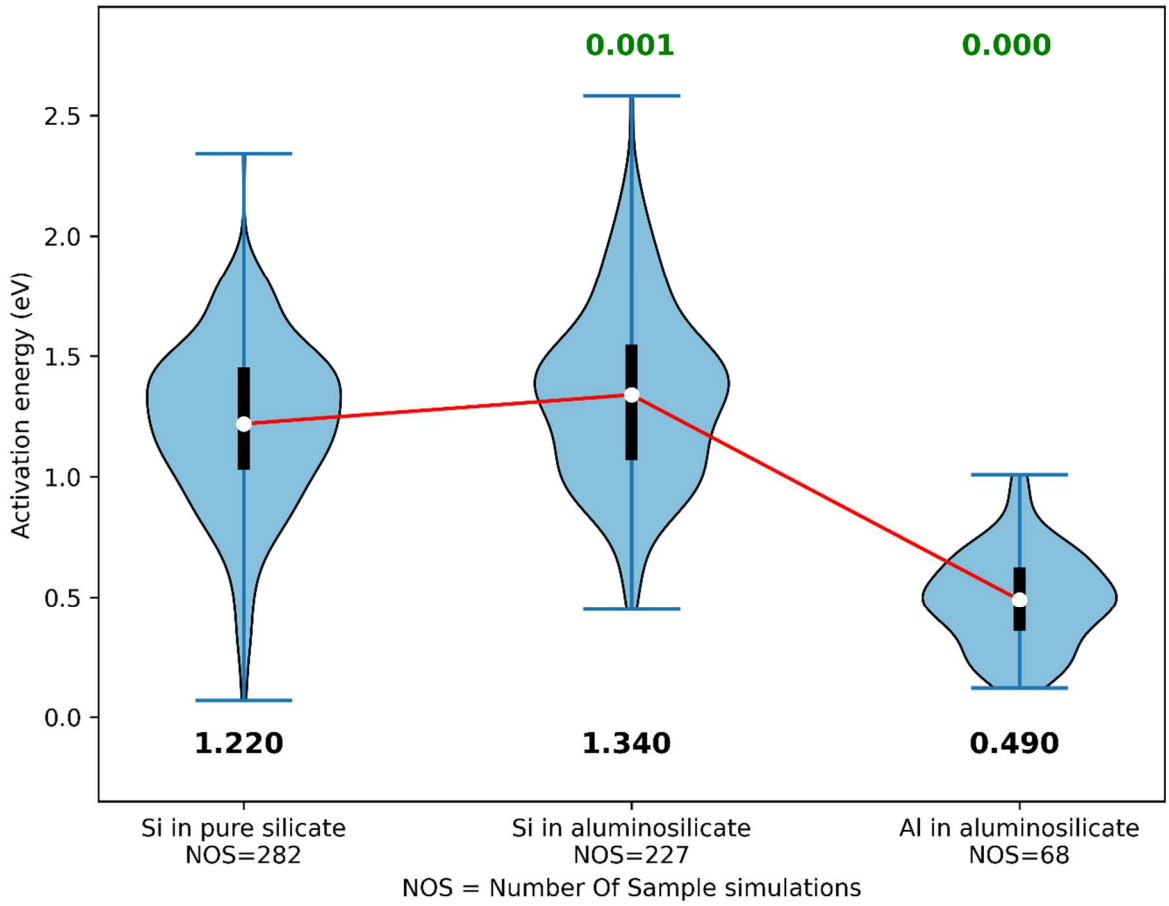

Figure 4. Distribution of activation energies for bond dissociation of Si in pure silicate, Si and Al in aluminosilicate glass. The blue violin shaped curve represents the distribution of data. Solid white circles represent the mean of the distribution, the red line connects the mean values and the black line represents the standard boxplot of Q1 – 25th percentile, Q3 – 75th percentile. The two whiskers extending the boxplot represent the standard boxplot minimum and maximum. Green coloured numbers on top of each violin plot represents the P-value with respect to the comparison of the first violin plot. Black coloured numbers below each violin plot represent the mean score in eV.

Table 1. XPS composition analysis of the ISG-Al-05 and ISG-Al-06 glasses before and after the alteration in distilled water.

Sample		Na	O	Ca	K	B	Zr	Si	Al	Al/Si
ISG-Al-05	**Theoretical composition**	11.4	57.8	1.6	-	9.2	0.5	13.1	6.4	**0.48**
	XPS before leaching	10.1	59.3	1.3	0.7	6.1	0.5	14.6	7.4	**0.51**
	XPS after leaching	8.7	63.2	0.5	0.8	-	1.2	18.7	6.9	**0.37**
	XPS variation before and after leaching (%)	-14%	7%	-62%	14%	-100%	140%	28%	-7%	**-27%**
ISG-Al-06	**Theoretical composition**	15.0	55.5	1.6	-	8.8	0.5	8.5	10.1	**1.18**
	XPS before leaching	11	58.3	1.3	1.2	5.8	0.5	10.6	11.4	**1.08**
	XPS after leaching	2.1	66.1	4.1	0.1	1.2	1.4	15.2	9.8	**0.64**
	XPS variation before and after leaching (%)	-81%	13%	215%	-92%	-79%	180%	43%	-14%	**-41%**

3.3 Experimental validation of the activation energies estimated through PMF calculations

XPS analysis was performed for the ISG-Al-05 (Si/Al=2.04) and ISG-Al-06 (Si/Al=0.5) glasses to record all the elemental compositions before and after leaching in distilled water with neutral pH in the range from 6.5 to 7.5 as shown in Table 1. A comparison between the Al/Si ratios recorded before and after the alteration directly indicates which element is preferentially dissolved from the glass and released into the solution. In pristine glass, Al/Si ratio of ISG-Al-05 and ISG-Al-06 are 0.51 and 1.08, respectively. After altering the top ~20 nm of glass, we observed that the Al/Si ratio drops by 27% in ISG-Al-05, whereas it drops by 41% in ISG-Al-06. This indicates that the addition of more Al into the glass leads to a faster dissolution of Al, which correlates with the activation energy of Al computed through PMF calculation being lower. The elemental composition depth profile of the altered layer formed on the ISG-Al-05 sample was obtained through the ToF-

SIMS profiling. The intensities were mean normalized with respect to the glass composition as shown in Figure 5. ToF-SIMS is comparatively less quantitative than XPS, but the first 5 nm data of the Al/Si ratio being consistent with XPS seems to increase the ToF-SIMS data reliability. The B profile indicates that the leaching of glass took place only within the first 20 nm, and retention of Na in the altered layer could possibly be due to charge compensation.

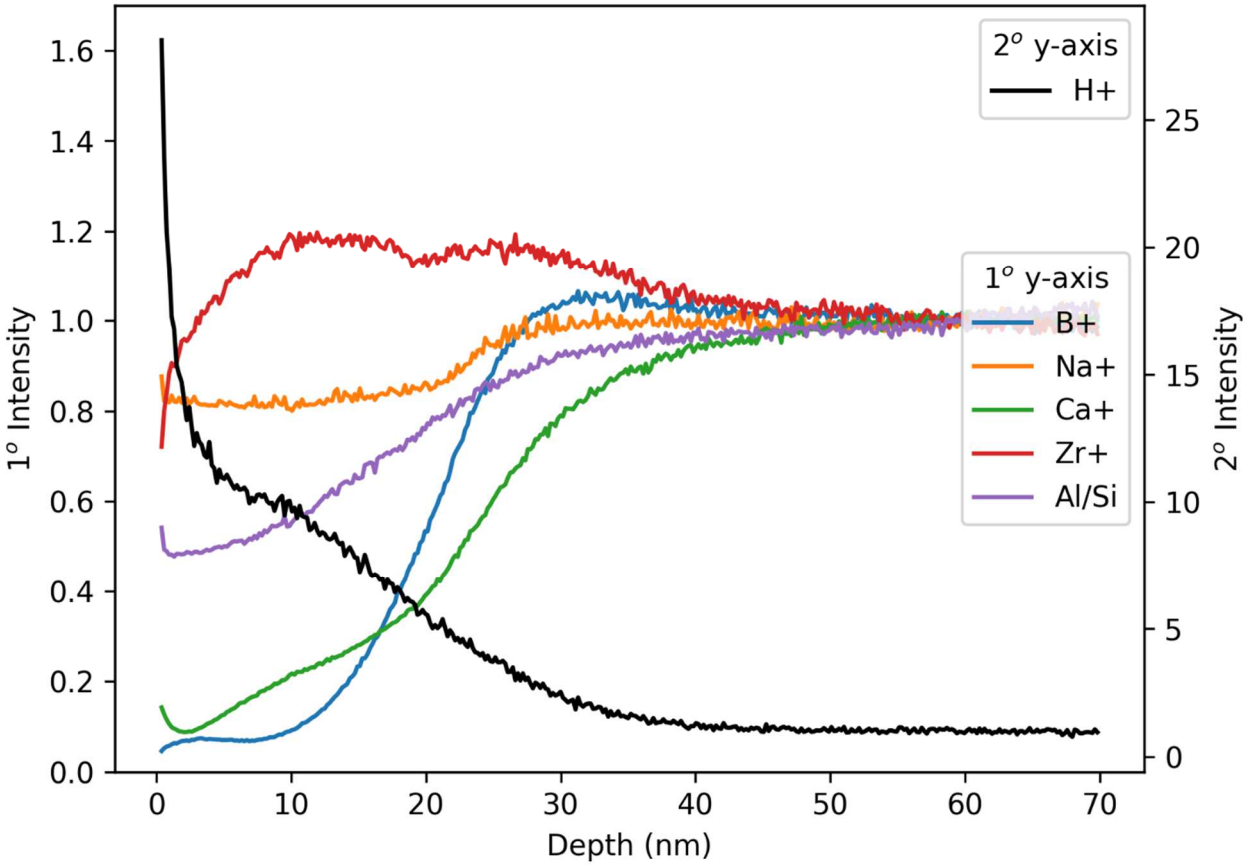

Figure 5. ToF-SIMS depth profiling of a coupon of ISG-AL-05 glass altered for 1 hr in deionized water at 90°C normalized to the mean of the pristine glass. The 1° *y*-axis in legend represents the primary *y*-axis, whose values correlated with the 1° intensity and the 2° *y*-axis represents the secondary *y*-axis, the H^+ data are to be correlated with the 2° intensity. The intensities are normalized to the mean of pristine glass.

The initial dissolution rate, r_0 measurements were performed through longer leaching tests with the ICP-OES analyses on the samples taken from the leachate at regular intervals. This parameter refers to the matrix dissolution, it is thus derived from the release of Si into the solution,

taking care that the solution remains sufficiently diluted to avoid feedback effects [51,52]. The results shown in Figure 6 indicate that r_0 is 64 times faster for the ISG-AL-06 glass than for the ISG-AL-05 glass. These results are in agreement with Hamilton's jadeite and nepheline glasses dissolution behaviour[26], where the glass with the lowest Si/Al ratio displays the fastest initial dissolution rate.

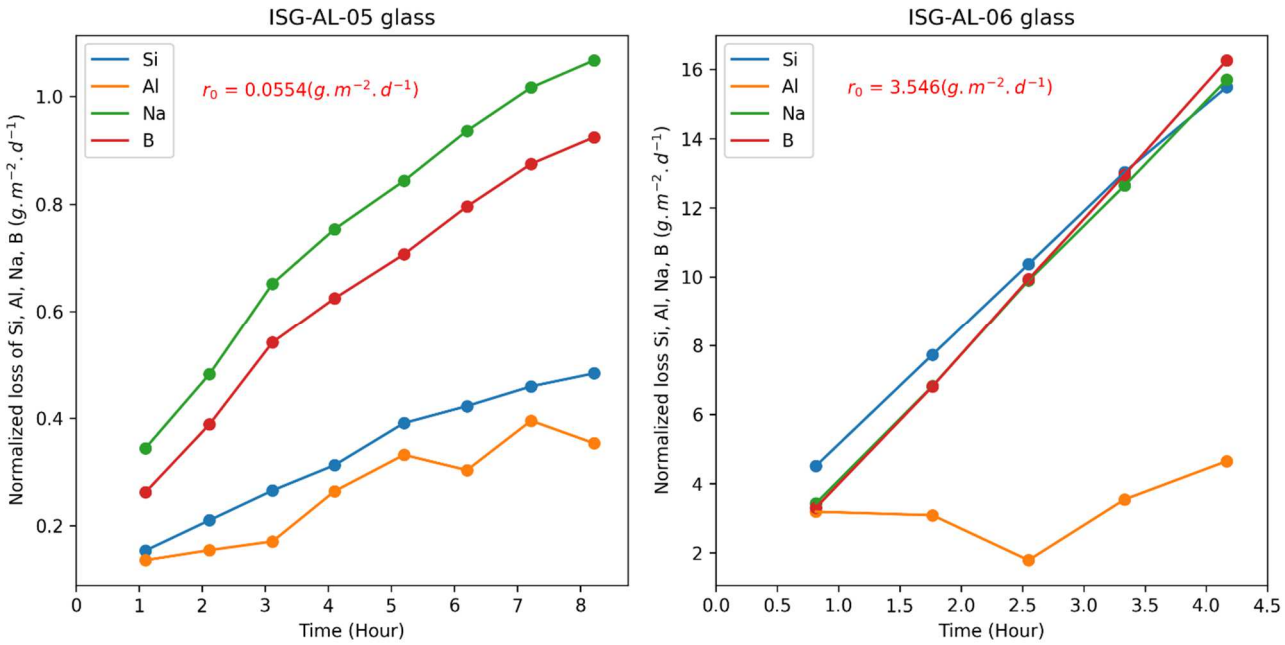

Figure 6. Initial dissolution rate of ISG-AL-05 and ISG-AL-06 glasses at 90°C and neutral pH. Blue – Si, orange – Al, green – Na, and red – Boron. Initial dissolution rate of Si is displayed in red colour text for both glasses.

Note that the preferential release of Al evidenced by the ToF-SIMS and XPS measurements cannot be seen here for several reasons: the uncertainties of the ICP-OES data are quite large (5% for Si and 10% for Al), the elemental concentrations in the onset solutions have not been measured, the alteration proceeds much deeper than for the solid-state characterization (300 nm in the case of ISG-AL-06) which could disturb Al release due to the reorganization of the Si-rich altered layer, and the leachate readily reaches saturation with respect to a low soluble Al-hydroxide mineral such as gibbsite, which explains the incongruency of the dissolution. For these reasons, monitoring the release rate of the various glass cations into the solution cannot be used to understand the processes

taking place at the atomistic scale. In conclusion, the experimental data provided here confirm that Al dissolves faster from the glass than Si, and that the glass with the highest Si/Al ratio has the lowest value of r_0, in agreement with Hamilton's results. It remains to understand how Al, when added at low concentration into the glass, increases the glass chemical durability.

3.4 Effects of the number of bridging oxygen atoms in pure silicate glass and of the local chemical environment of aluminosilicate glass on the activation barrier

Recent study has shown that the activation energy required to dissociate the bonds around the Si atoms changes with the number of bridging oxygens to the target atom[11]. Therefore, we have statistically investigated the possible correlation between the number of bridging oxygens to the target atom with their corresponding dissociation energies of the bonds. The distribution of activation energies required to dissociate the bonds around Si atoms in pure silicate glass based on the number of bridging oxygens in Si coordination is shown in Figure 7a. Analysing the activation energies for more than 100 data points indicates that the mean energy required to dissociate a bond to change a SiP3 into a SiP2 species is higher than the one necessary to dissociate a bond to change a SiP4 into a SiP3 speices. (Here SiP4 means Si in Pure silicate with 4 bridging oxygens. Similarly, SiA4 and AlA4 will be used to represent Si and Al in Aluminosilicate glass, respectively, with 4 bridging oxygens).

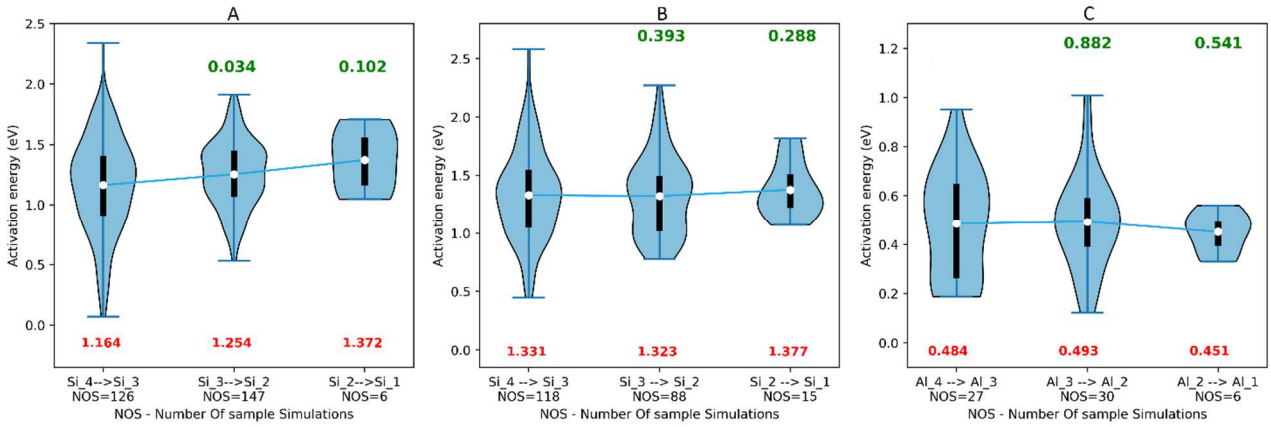

Figure 7. Distributions of the activation energies for bond dissociation of Si in pure silicate (A), Si in aluminosilicate glass (B), and Al in aluminosilicate glass (C), each categorized based on the number of bridging oxygens. The violin shaped curves represent the distribution of the data points. Solid white circles represent the mean of the distribution, blue line connects the mean values, and

black line represents the standard boxplot of Q1 – 25th percentile, Q3 – 75th percentile. The two whiskers extending the boxplot represent the standard boxplot minimum and maximum. Green numbers on top of each violin plot represent the p-values with respect to a comparison with the first violin plot. Red numbers below each violin plot represent the mean score. On the *x*-axis, for instance, Si_4 → Si_3 means that the target atom Si with initially 4 bridging oxygens, becomes coordinated with three bridging oxygens after dissociation by water.

With the Kolmogorov-Smirnov test, both of these data sets are not normally distributed. (Their p-values are given in the Table A2 of the Appendices). Therefore, we proceed to conduct the non-parametric MWU test to investigate if the two means are significantly different or not. Interestingly, we found the p-value to be 0.034, indicating that a dissociation of a SiP3 species requires significantly more energy than a dissociation of a SiP4 species.

Similarly, we can classify the activation energies for the bonds around the Si and Al atoms in the aluminosilicate glass based on the number of bridging oxygens in their coordination (Figure 7). We note that the mean activation energy required to dissociate a bond around the SiA4 species is as strong as that for the SiA3 species for dissociating a bond around a Si atom in aluminosilicate glass. Additionally, both of these activation energies are above 1.3 eV, which is higher than what is observable for the SiP3 and SiP4 species in pure silicate glass. Therefore, the rate limiting step for the dissolution of aluminosilicate glass starts from SiA4 species and continues with SiA3 species, whereas pure silicate is rate limiting only starting from the SiP3 species.

To understand the reason for a higher strength of the SiA4 species, we investigated the effects of the local environment on the dissociation energies around Si atoms in the aluminosilicate glass. We categorized them using the activation energy based on their coordination with the number of Al atoms as their second neighbours. Interestingly, when the second neighbours of the target Si atom do not contain Al, its average activation energy was 1.23 eV, which is less than for the SiP3 species, but the presence of single Al as a second neighbour increased the activation energy to 1.35 eV and further to 1.42 eV for two Al as second neighbours, as shown in Figure 8A.

The species Al_0, Al_1 and Al_2 have more data to rely upon their significance, but beyond them the number of data points is less. Nevertheless, it is very clear that a Si species in aluminosilicate glass with no Al as a second neighbour is easier to dissociate than a Si species with Al as a second neighbour. This indicates that Al has a significant local effect on the Si to strengthen the glass, which is responsible for rise in activation energy. In oxide glasses, Al atom has always been of great interest for its ability to increase the polymerization of the glass structure due to its network-forming role[50] and the reduction of the non-bridging oxygen content with the formation of negatively charged $[AlO_{4/2}]^{-1}$ tetrahedral units, charge balanced by modifiers[53]. Therefore, despite Al being such a weak element with low activation energy, Al atom increases the network connectivity of glass by making more SiA4 species (which is stronger than SiP4 or SiP3), and so these indirect benefits outweigh the easier dissolution of the Al atom. Finally, the mystery appears to be solved that the Al itself is not the strong element in aluminosilicate glass, but it plays a vital role in strengthening the major element Si to increase the durability of the glass, which is in agreement with the XPS results and ToF-SIMS data.

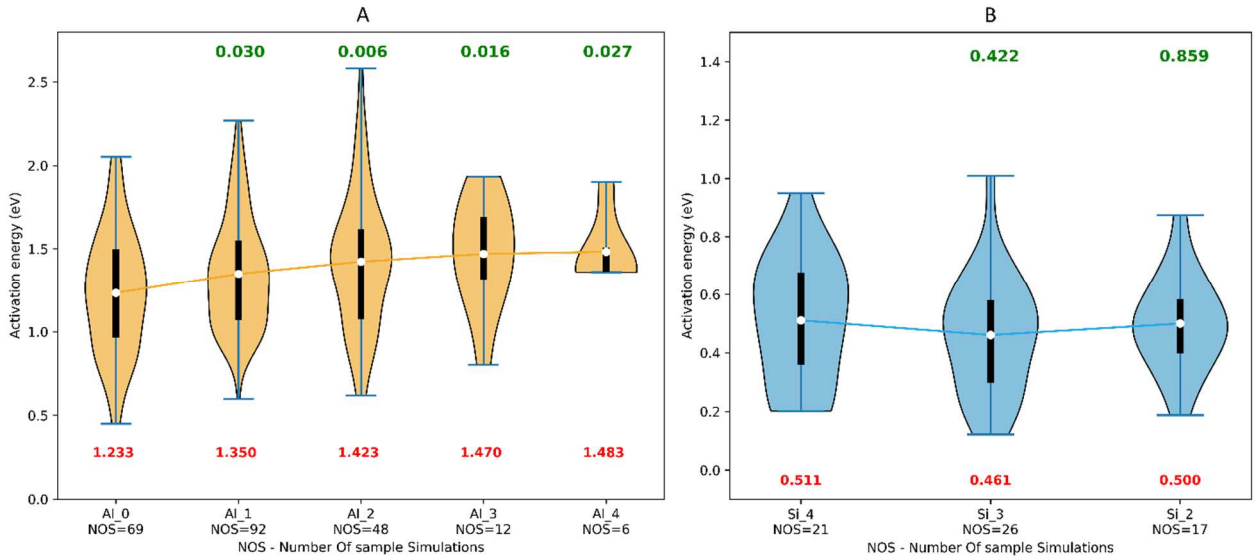

Figure 8. Distribution of the activation energies for bond dissociation: (A) Si in aluminosilicate glass based on the presence of Al as second neighbours; (B) Al in aluminosilicate glass based on the presence of Si as second neighbours. The violin shaped curves represent the distribution of data points. Solid white circles represent the mean of the distribution, red line (A) and blue line (B) connect the mean values. The black boxplots represent Q1 – 25th percentile and Q3 – 75th

percentile. The two whiskers extending the boxplots represent standard boxplot minimum and maximum. Green numbers on top of the each violin shape represents the p-values with respect to a comparison with the first violin plot. Red numbers below each violin plot represent the mean score. For figure (A), on the *x*-axis, Al_0 represents no Al as a second neighbour for the target Si atom, and extends through Al_1, Al_2, Al_3 up to Al_4 indicating four Al as second neighbours. For figure (B), on the *x*-axis, Si_4 represents 4 Si as second neighbours for the target Al atom, up to Si_2 having two Si as second neighbours.

3.5 Correlating the structural features of the glass with the activation energies

Chemical composition determines the structure and mechanical properties[54], both of which, in turn, control the durability of the glass[21,55]. Therefore, we investigated if there is any correlation between the structural properties like bond angles or the mechanical properties like the local stress tensors (hydrostatic pressure and shear) with the activation energies for the bond dissociation of Si–O–Si bridges in pure silica, and Si–O–X or Al–O–X bridges in the aluminosilicate glass. The calculated bond angles of the three-atom bridge dissociated by water are in the range of 115° to 180° for pure silicate, whereas in the aluminosilicate glass, the average bond angles are a little lower:
Si–O–Si (150°), Si–O–Al (135°), Al–O–Si (139°), and Al–O–Al (135°). Regression analysis performed to correlate these structural features against activation energies are shown in Figure 9, and indicates that the activation energy required for dissociating the bond increases with increasing the bond angle. The hypothesis with 95% confidence interval has been tested statistically and it is found that the activation energy depends on the bond angle for Si in pure silicate and Si, Al in aluminosilicate glass with the p-values less than 0.05 (Table A7 Appendices).

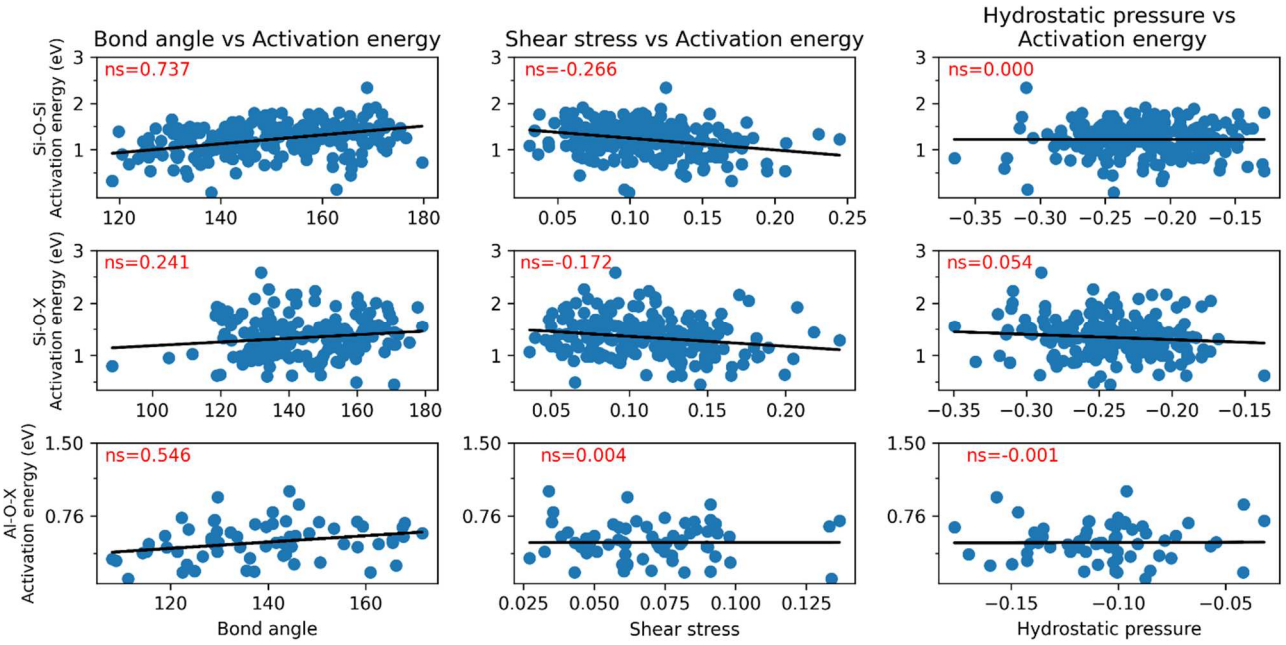

Figure 9. Correlation of the bond angle, shear stress and hydrostatic pressure with the activation energy for Si in pure silicate, Si and Al in aluminosilicate glass. Data points are represented by blue dots, and the regression black lines are fits to the data. The scale of bond length is 100 times of its activation energy, so both the x-axis values and the y-axis values for all plots are divided by their respective maximum values to normalize both x and y-axes and then slope is calculated to represent as NS – Normalized slope. Three plots in the first column are the correlations of the bond angle *vs* activation energy, the second column shows the correlations of the Shear stress *vs* activation energy, and the third column shows the Hydrostatic pressure *vs* activation energy correlation.

Then linear regression for the local shear stress *vs* activation energy revealed that increasing the shear stress decreases the activation energy. By statistically testing this hypothesis, the existence of this correlation is confirmed in pure silicate and in the aluminosilicate glasses (bonds around Si), but not for the bonds around the Al in the aluminosilicate glass. On the other hand, the linear regression of hydrostatic pressure with hypothesis testing shows that there is no significant correlation between the local hydrostatic pressure and the activation energy for the bonds around the Si, Al atoms in the aluminosilicate glass and around Si in pure silicate glass. However, the distribution of local hydrostatic pressures for Si in the aluminosilicate glass is more skewed towards negative than for Si in pure silicate, probably because of the lower number of non-bridging oxygens around the tetra-coordinated Si. As we can see in Figure 9, not all the points are closely fitted by a

straight line; rather we are just able to observe a certain trend for all three parameters. This is because several structural features simultaneously control the activation energy required by the water molecule to dissociate the bridges, and not only one. Nevertheless, these results indicate that the bond angle and the local shear stress have a larger effect on the activation energy, while the local hydrostatic pressure is not affecting the dissociation of bonds in silicate and aluminosilicate glass.

4 DISCUSSION

The durability of the silicate glass against water is increased by the addition of a small amount of Al in the CJ2 type of glass[9]. However, in our study, surprisingly, the average activation energy necessary to break a bond around one Al atom in an aluminosilicate glass is estimated to be just 0.49 eV. This is not even half of the energy required to dissociate a bond around one Si atom in pure silicate glass. These results are in agreement with experimental data obtained from solid state characterization at a nanometer scale with XPS and ToF-SIMS on two model aluminosilicate glasses. Statistically, it is found that the energy required to dissociate a bond around Si atom in the aluminosilicate glass is significantly higher than in pure silicate glass. This indicates that the addition of Al strengthens the bonds around Si atoms in the glass. Interestingly, a Si atom surrounded by four bridging oxygens (SiP4) in pure silicate glass is weaker than a Si atom surrounded by three bridging oxygens and one non-bridging oxygen (SiP3) in the same glass and the difference is statistically significant. This is in agreement with previous studies on water dissociating the silicate glass by PMF method for a small number of samples[11]. It is important to notice the activation energy estimated in reference [11] is in range between 0.17eV to 0.95eV which is different from the range in our study. It seems that a water molecule approaching the reaction site with a specific orientation modifies the energy barriers. In reference [11], the authors have chosen one particular orientation for the water molecule to target the silicate bond. And this orientation corresponds to the easiest way to break the Si-O-Si bond. It is interesting to notice that we measured

some activation energies in the regime from 0.1ev to 0.95eV. Additionally, we also observed the same mechanism as theirs. i.e.,

1. In our study, it seems that the water molecule dissociates the back siloxane bridge is same as in Figure 1 of the reference [11].

2. The mechanism of higher activation barrier for SiP3 than SiP4.

However, we observed much broader regime for activation energy as we did not change the orientation of every water molecules against the Si-O-Si bond. Therefore, the scale of activation energy is slightly different between the two studies yet the mechanisms understood remains the same.

We also found that, the bonds around the Si surrounded by four bridging oxygens (SiA4) in the aluminosilicate glass are as strong as the ones around the Si surrounded by three bridging oxygens and one non-bridging oxygen (SiA3), and additionally both activation energies are higher than for the SiP3 and SiP4 species. Investigating the reason for such rise in the activation barrier revealed that when there is no Al as a second neighbour around a Si atom in aluminosilicate glass, its activation energy is very close to SiP. However, in the presence of one or two Al atoms connected as second neighbours, the activation barrier for Si becomes significantly higher which indicates that it is exactly the presence of Al in the local environment that is actually responsible for this rise. Recent abinitio study associated with metadynamics has also found that activation energy required to break the Si-O-Al bridge is higher than dissociating Si-O-Si[56], which supports our results. The scale of activation barriers in Dupuis et al.'s study[56] is very different from our study because they worked with short silicate chains and that could modify the activation barrier. In fact Pelmenschikov et al. [57] have observed that activation barrier increases when Si-O-Si has more constraints nearby, and vice versa. It is also important to note that the content of SiA4 species in the aluminosilicate glass is larger than SiP4 in pure silicate glass because Al increases the polymerization of the network. Therefore, addition of Al is strengthening the bonds around the

major glass-forming element, i.e. Si, and these features differing from the pure silicate glass is what increases the durability of the aluminosilicate glass.

This type of chemical reactions between water and silicate systems can also be studied through the ReaxFF force field [58]. Some recent studies used the advantage of the ReaxFF potential associated with parallel tempering method[59] or high temperature MD method[60] to accelerate the mechanisms of bond formation or dissociation to better understand the silicate gel formation or evolution of these gels by chemical attacks. However, in our study, we were particularly interested in estimating the activation barrier for silicate dissolution reaction at 300K with very large statistics to understand the relation between the glass structure and the durability against water. So we chose here the classical reactive potential developed by Mahadevan-Garofalini (MG)[36,61,62]. It is estimated that MG forcefield is atleast ten times faster than a similar ReaxFF calculation[61]. The development of MG potential is inspired by the concept of varying the ion charge as function of the distance[63], fitted through quantum mechanical calculations. They added intramolecular interactions along with two - and three-body terms, to allow the water for dissociation of the silicate molecule[62]. It is very important to notice, this reactive potential was evaluated [64], and found very well comparable with the ReaxFF potentials. Later the authors improved this potential for sodium silicate glasses[61], which is also found to be very well in agreement with the available experimental structural information. More recently, a reactive potential for more complex systems was developed and validated with the inclusion of SiO_2-Al_2O_3-CaO + H_2O set of parameters [36]. It is why we chose the MG potential for generating the large statistical dataset to investigate the glass structural parameters and the activation barriers.

Recent study has found that the glass dissolution rate drops significantly with the addition of a small quantity of Al to silicate glass (< 3.5%), and the decline rate of glass dissolution becomes gradual at intermediate concentration of Al (3.5%-19%)[27]. However, the addition of more than 19% of alumina triggers a significant rise of the dissolution rate of the glass[27]. The statistical PMF simulation results in our study are explaining quite well the possible atomistic mechanism

behind the role of Al towards dissolution rate of the glass. The incorporation of a small quantity of Al in the glass increases its durability. See, for instance the CJ1 glass (with no Al) with an initial dissolution rate 4 times larger than for the CJ2 glass (containing 4% Al)[9]. Despite Al has less activation energy and being weak element to easily dissociate from the glass, it increases the polymerization of the network resulting in the introduction of more Si with 4 bridging oxygens. Additionally, Al being a second neighbour strengthens the bond around Si in the glass. Both mechanisms together outweigh the low activation energy of Al and make the CJ2 type of glasses to be more durable.

Al at intermediate concentration (3.5%-19%), this regime from the mid towards 3.5% converts three co-ordinated Si to become four co-ordinated Si surrounded by Al as second neighbour. The concentration regime from the mid towards the 19% involves in preferential dissolution of Al, which weakens the silicate network due to the percolation of the bonds containing the Al, so the decline rate of dissolution becomes gradual when the Al percentage exceeds a critical value. The addition of Al at high concentrations makes the dissolution of Al too much preferential, which completely weakens the silicate network. Under these circumstances, the low activation energy of Al becomes dominant over the two strengthening mechanisms of Al, which totally collapse the durability of the glass. This effect has been observed for our two model glasses and in the literature data on plagioclase glasses[26].

It has been reported previously that the addition of Al to pure silicate glass increases the durability by two mechanisms. The first mechanism is by reducing the Na coordination with non-bridging oxygen (weak) and increasing the coordination of Na with Al (strong). The second mechanism is by increasing the connectivity of the glass network, which appropriately reduces the diffusion of water[13]. Between these two mechanisms, our simulation results, along with the previous experimental results[27], propose that the second mechanism plays a dominant role in improving the durability of glass over the first mechanism.

With respect to the first mechanism, increasing the Al content in glass will decrease the Na coordinated to non-bridging oxygens (Na is easier to dissociate when coordinated with non-bridging oxygen). However, with respect to the second mechanism, Al increases the network connectivity, increases the strength of Si through local effects, and so reduces the diffusion rate through hydrolysis processes of water molecule inside the glass. For these reasons, following this study, Al strengthening a major glass-forming element like Si is considered as the main contributing factor towards the durability of glass and so the second mechanism plays dominant role over the first mechanism.

In recent years, traditional "trial-and-error" methods to design the glasses are replaced with artificial intelligence to accelerate the discovery of advanced materials[65–67]. Current machine learning models for predicting the dissolution kinetics of the glass are trained with input data such as the composition of the glass, pH of the solution, and their corresponding dissolution rates observed experimentally[68,69]. However, there is a lack of data to understand in detail the relationships between the composition, structure, and durability. The automated pipeline designed in our study takes the composition as an input and provides structural information of the atom (the number of bridging oxygens, bond angles, local hydrostatic pressure and shear stress, etc.) with their corresponding activation energies as an output. The statistical analysis revealed the role of Al towards the increased durability of aluminosilicate glass. The correlation of our simulation data with experimental results provides more confidence to the simulations reliability, and the use of classical potentials to perform such simulations makes it computationally affordable to generate large amounts of data. This method cannot be limited to pure silicate and aluminosilicate glasses, but can also be extended to include Na, Mg or B into the glass composition to investigate more complex and more realistic glass compositions. Therefore, we believe that this method of automated pipeline to create the wide set of data on composition-structure-durability interdependencies along with experimental dissolution analysis of extreme compositions would be a promising fast method to develop a strong machine-learning model in glass science.

5 CONCLUSIONS

Al causes opposing effects on glass durability against water when added at low and high concentrations. To reveal the structural mechanism behind this behaviour, it is very important to understand the correlation between local structural features of the glass and the activation energies of individual bonds. However, finding the correlation between these two parameters is very complicated because the range of activation energies for bond dissociation is very narrow with large standard deviations. In this study, we overcome this difficulty by estimating the activation energy barrier for a statistically large set of configurations to understand their relation with local structural features. The calculated PMF results along with experimental data revealed that it is very easy to dissociate Al from the glass and found with statistical significance that dissociating Si from aluminosilicate glass is much more difficult than dissociating Si from pure silicate glass. Further investigation of the local environment of Si in aluminosilicate glass has shown that the activation barrier for Si dissolution is significantly increases by the presence of Al as a second neighbour. As a result, the addition of Al in small concentration increases the durability by reinforcing the strength of Si and increasing the polymerization of the glass network. Whereas at high Al concentration, the preferential release of Al results in the weakening of the silicate network and so the durability of plagioclase-type mineral glasses decreases with increasing Al concentration. The developed methodology has helped us in understanding the role of Al in silicate glasses, but can also be extended to include Na, Mg, or B for the investigation of more complex glass compositions. Generating huge data sets of structural features with their corresponding activation energies for all the glass elements will serve as an input for developing a strong machine-learning tool, which will help us to design the glass compositions to obtain the desired quality glass quickly.

6 Acknowledgement

Authors are grateful to Benjamin Parruzot and Joelle Reiser (Pacific Northwest National Laboratory, USA) for supplying us with ISG-AL-05 and ISG-AL-06 samples. They are also grateful to Elodie Chauvet, Loan Lai, Charbel Roukkos and Yves Depuidt at TESCAN ANALYTICS, France, for conducting the XPS and ToF-SIMS analysis.

This study was supported as part of the Center for Performance and Design of Nuclear Waste Forms and Containers, U.S. Department of Energy (DOE) [#DESC0016584];

7 REFERENCES

[1] Y. Xiang, J. Du, M.M. Smedskjaer, J.C. Mauro, Structure and properties of sodium aluminosilicate glasses from molecular dynamics simulations, J. Chem. Phys. 139 (2013) 044507. https://doi.org/10.1063/1.4816378.

[2] S. Petitgirard, C.J. Sahle, C. Weis, K. Gilmore, G. Spiekermann, J.S. Tse, M. Wilke, C. Cavallari, V. Cerantola, C. Sternemann, Magma properties at deep Earth's conditions from electronic structure of silica, Geochem. Perspect. Lett. (2019) 32–37. https://doi.org/10.7185/geochemlet.1902.

[3] C. Cailleteau, F. Angeli, F. Devreux, S. Gin, J. Jestin, P. Jollivet, O. Spalla, Insight into silicate-glass corrosion mechanisms, Nat. Mater. 7 (2008) 978–983. https://doi.org/10.1038/nmat2301.

[4] E.M. Pierce, B.P. McGrail, P.F. Martin, J. Marra, B.W. Arey, K.N. Geiszler, Accelerated weathering of high-level and plutonium-bearing lanthanide borosilicate waste glasses under hydraulically unsaturated conditions, Appl. Geochem. 22 (2007) 1841–1859. https://doi.org/10.1016/j.apgeochem.2007.03.056.

[5] L.R. Kump, S.L. Brantley, M.A. Arthur, Chemical Weathering, Atmospheric CO_2, and Climate, Annu. Rev. Earth Planet. Sci. 28 (2000) 611–667. https://doi.org/10.1146/annurev.earth.28.1.611.

[6] G.E. Hilley, S. Porder, A framework for predicting global silicate weathering and CO2 drawdown rates over geologic time-scales, Proc. Natl. Acad. Sci. 105 (2008) 16855–16859. https://doi.org/10.1073/pnas.0801462105.

[7] S. Gin, A. Abdelouas, L.J. Criscenti, W.L. Ebert, K. Ferrand, T. Geisler, M.T. Harrison, Y. Inagaki, S. Mitsui, K.T. Mueller, J.C. Marra, C.G. Pantano, E.M. Pierce, J.V. Ryan, J.M. Schofield, C.I. Steefel, J.D. Vienna, An international initiative on long-term behavior of high-level nuclear waste glass, Mater. Today. 16 (2013) 243–248. https://doi.org/10.1016/j.mattod.2013.06.008.

[8] M. Ojovan, W. Lee, S. Kalmykov, An Introduction to Nuclear Waste Immobilisation - 3rd Edition, (2019). https://www.elsevier.com/books/an-introduction-to-nuclear-waste-immobilisation/ojovan/978-0-08-102702-8 (accessed June 11, 2021).

[9] S. Gin, A.H. Mir, A. Jan, J.M. Delaye, E. Chauvet, Y. De Puydt, A. Gourgiotis, S. Kerisit, A General Mechanism for Gel Layer Formation on Borosilicate Glass under Aqueous Corrosion, J. Phys. Chem. C. 124 (2020) 5132–5144. https://doi.org/10.1021/acs.jpcc.9b10491.

[10] B. Grambow, Nuclear Waste Glasses - How Durable?, Elements. 2 (2006) 357–364. https://doi.org/10.2113/gselements.2.6.357.

[11] M. Kagan, G.K. Lockwood, S.H. Garofalini, Reactive simulations of the activation barrier to dissolution of amorphous silica in water, Phys Chem Chem Phys. 16 (2014) 9294–9301. https://doi.org/10.1039/C4CP00030G.
[12] G. Perera, R.H. Doremus, W. Lanford, Dissolution Rates of Silicate Glasses in Water at pH 7, J. Am. Ceram. Soc. 74 (1991) 1269–1274. https://doi.org/10.1111/j.1151-2916.1991.tb04096.x.
[13] B.M.J. Smets, M.G.W. Tholen, Leaching of Glasses with Molar Composition 20Na2O · 10RO ·x Al2O3· (70-x)SiO2, J. Am. Ceram. Soc. 67 (1984) 281–284. https://doi.org/10.1111/j.1151-2916.1984.tb18848.x.
[14] B.P. McGrail, J.P. Icenhower, D.K. Shuh, P. Liu, J.G. Darab, D.R. Baer, S. Thevuthasen, V. Shutthanandan, M.H. Engelhard, C.H. Booth, P. Nachimuthu, The structure of Na2O–Al2O3–SiO2 glass: impact on sodium ion exchange in H2O and D2O, J. Non-Cryst. Solids. 296 (2001) 10–26. https://doi.org/10.1016/S0022-3093(01)00890-0.
[15] J.J. Neeway, P.C. Rieke, B.P. Parruzot, J.V. Ryan, R.M. Asmussen, The dissolution behavior of borosilicate glasses in far-from equilibrium conditions, Geochim. Cosmochim. Acta. 226 (2018) 132–148. https://doi.org/10.1016/j.gca.2018.02.001.
[16] B. Grambow, R. Müller, First-order dissolution rate law and the role of surface layers in glass performance assessment, J. Nucl. Mater. 298 (2001) 112–124. https://doi.org/10.1016/S0022-3115(01)00619-5.
[17] T. Geisler, T. Nagel, M.R. Kilburn, A. Janssen, J.P. Icenhower, R.O.C. Fonseca, M. Grange, A.A. Nemchin, The mechanism of borosilicate glass corrosion revisited, Geochim. Cosmochim. Acta. 158 (2015) 112–129. https://doi.org/10.1016/j.gca.2015.02.039.
[18] G.S. Frankel, J.D. Vienna, J. Lian, X. Guo, S. Gin, S.H. Kim, J. Du, J.V. Ryan, J. Wang, W. Windl, C.D. Taylor, J.R. Scully, Recent Advances in Corrosion Science Applicable To Disposal of High-Level Nuclear Waste, Chem. Rev. (2021) acs.chemrev.0c00990. https://doi.org/10.1021/acs.chemrev.0c00990.
[19] S. Gin, J.-M. Delaye, F. Angeli, S. Schuller, Aqueous alteration of silicate glass: state of knowledge and perspectives, Npj Mater. Degrad. 5 (2021) 42. https://doi.org/10.1038/s41529-021-00190-5.
[20] S. Gin, Open Scientific Questions about Nuclear Glass Corrosion, Procedia Mater. Sci. 7 (2014) 163–171. https://doi.org/10.1016/j.mspro.2014.10.022.
[21] G.S. Frankel, A comparative review of the aqueous corrosion of glasses, crystalline ceramics, and metals, Npj Mater. Degrad. (2018) 17.
[22] Q. Zheng, M.M. Smedskjaer, R.E. Youngman, M. Potuzak, J.C. Mauro, Y. Yue, Influence of aluminum speciation on the stability of aluminosilicate glasses against crystallization, Appl. Phys. Lett. 101 (2012) 041906. https://doi.org/10.1063/1.4739005.
[23] M.M. Smedskjaer, L. Huang, G. Scannell, J.C. Mauro, Elastic interpretation of the glass transition in aluminosilicate liquids, Phys. Rev. B. 85 (2012) 144203. https://doi.org/10.1103/PhysRevB.85.144203.
[24] J.C. Mauro, M.M. Smedskjaer, Statistical mechanics of glass, J. Non-Cryst. Solids. 396–397 (2014) 41–53. https://doi.org/10.1016/j.jnoncrysol.2014.04.009.
[25] L. Wondraczek, J.C. Mauro, J. Eckert, U. Kühn, J. Horbach, J. Deubener, T. Rouxel, Towards Ultrastrong Glasses, Adv. Mater. 23 (2011) 4578–4586. https://doi.org/10.1002/adma.201102795.
[26] J.P. Hamilton, S.L. Brantley, C.G. Pantano, L.J. Criscenti, J.D. Kubicki, Dissolution of nepheline, jadeite and albite glasses: toward better models for aluminosilicate dissolution, Geochim. Cosmochim. Acta. 65 (2001) 3683–3702. https://doi.org/10.1016/S0016-7037(01)00724-4.
[27] J.D. Vienna, J.V. Crum, Non-linear effects of alumina concentration on Product Consistency Test response of waste glasses, J. Nucl. Mater. 511 (2018) 396–405. https://doi.org/10.1016/j.jnucmat.2018.09.040.

[28] L.J. Criscenti, J.D. Kubicki, S.L. Brantley, Silicate Glass and Mineral Dissolution: Calculated Reaction Paths and Activation Energies for Hydrolysis of a Q^3 Si by H_3O^+ Using Ab Initio Methods, J. Phys. Chem. A. 110 (2006) 198–206. https://doi.org/10.1021/jp044360a.
[29] J.E. Del Bene, K. Runge, R.J. Bartlett, A quantum chemical mechanism for the water-initiated decomposition of silica, Comput. Mater. Sci. 27 (2003) 102–108. https://doi.org/10.1016/S0927-0256(02)00432-9.
[30] Y. Xiao, A.C. Lasaga, Ab initio quantum mechanical studies of the kinetics and mechanisms of silicate dissolution: H +(H30 ') catalysis, Geochim. Cosmochim. Acta. 58 (1994) 5379–5400.
[31] J.P. Icenhower, P.M. Dove, The dissolution kinetics of amorphous silica into sodium chloride solutions: effects of temperature and ionic strength, Geochim. Cosmochim. Acta. 64 (2000) 4193–4203. https://doi.org/10.1016/S0016-7037(00)00487-7.
[32] A. Pelmenschikov, J. Leszczynski, L.G.M. Pettersson, Mechanism of Dissolution of Neutral Silica Surfaces: Including Effect of Self-Healing, J. Phys. Chem. A. 105 (2001) 9528–9532. https://doi.org/10.1021/jp011820g.
[33] A.F. Wallace, G.V. Gibbs, P.M. Dove, Influence of Ion-Associated Water on the Hydrolysis of Si−O Bonded Interactions, J. Phys. Chem. A. 114 (2010) 2534–2542. https://doi.org/10.1021/jp907851u.
[34] H. Xu, J.S.J. Van Deventer, Ab initio calculations on the five-membered alumino-silicate framework rings model: implications for dissolution in alkaline solutions, Comput. Chem. 24 (2000) 391–404. https://doi.org/10.1016/S0097-8485(99)00080-7.
[35] I.T. Todorov, W. Smith, K. Trachenko, M.T. Dove, DL_POLY_3: new dimensions in molecular dynamics simulations via massive parallelism, J. Mater. Chem. 16 (2006) 1911. https://doi.org/10.1039/b517931a.
[36] T.S. Mahadevan, J. Du, Atomic and micro-structure features of nanoporous aluminosilicate glasses from reactive molecular dynamics simulations, J. Am. Ceram. Soc. 104 (2021) 229–242. https://doi.org/10.1111/jace.17465.
[37] D. Wolf, P. Keblinski, S.R. Phillpot, J. Eggebrecht, Exact method for the simulation of Coulombic systems by spherically truncated, pairwise r−1 summation, J. Chem. Phys. 110 (1999) 8254–8282. https://doi.org/10.1063/1.478738.
[38] A. Jan, J.-M. Delaye, S. Gin, S. Kerisit, Molecular dynamics simulation of ballistic effects in simplified nuclear waste glasses, J. Non-Cryst. Solids. 505 (2019) 188–201. https://doi.org/10.1016/j.jnoncrysol.2018.11.021.
[39] H.J.C. Berendsen, J.R. Grigera, T.P. Straatsma, The missing term in effective pair potentials, J. Phys. Chem. 91 (1987) 6269–6271. https://doi.org/10.1021/j100308a038.
[40] J.A. Zimmerman, E.B. WebbIII, J.J. Hoyt, R.E. Jones, P.A. Klein, D.J. Bammann, Calculation of stress in atomistic simulation, Model. Simul. Mater. Sci. Eng. 12 (2004) S319–S332. https://doi.org/10.1088/0965-0393/12/4/S03.
[41] M. Zhou, A new look at the atomic level virial stress: on continuum-molecular system equivalence, Proc. R. Soc. Lond. Ser. Math. Phys. Eng. Sci. 459 (2003) 2347–2392. https://doi.org/10.1098/rspa.2003.1127.
[42] P. Mishra, C.M. Pandey, U. Singh, A. Gupta, C. Sahu, A. Keshri, Descriptive Statistics and Normality Tests for Statistical Data, Ann. Card. Anaesth. 22 (2019) 67–72. https://doi.org/10.4103/aca.ACA_157_18.
[43] N. Mohd Razali, B. Yap, Power Comparisons of Shapiro-Wilk, Kolmogorov-Smirnov, Lilliefors and Anderson-Darling Tests, J Stat Model Anal. 2 (2011).
[44] S. Parab, S. Bhalerao, Choosing statistical test, Int. J. Ayurveda Res. 1 (2010) 187–191. https://doi.org/10.4103/0974-7788.72494.
[45] X. Lu, J.T. Reiser, B. Parruzot, L. Deng, I.M. Gussev, J.C. Neuefeind, T.R. Graham, H. Liu, J.V. Ryan, S.H. Kim, N. Washton, M. Lang, J. Du, J.D. Vienna, Effects of Al:Si and (Al + Na):Si ratios on the properties of the international simple glass, part II: Structure, J. Am. Ceram. Soc. 104 (2021) 183–207. https://doi.org/10.1111/jace.17447.

[46] J.T. Reiser, X. Lu, B. Parruzot, H. Liu, T. Subramani, H. Kaya, R.M. Kissinger, J.V. Crum, J.V. Ryan, A. Navrotsky, S.H. Kim, J.D. Vienna, Effects of Al:Si and (Al + Na):Si ratios on the properties of the international simple glass, part I: Physical properties, J. Am. Ceram. Soc. 104 (2021) 167–182. https://doi.org/10.1111/jace.17449.
[47] M. Collin, S. Gin, P. Jollivet, L. Dupuy, V. Dauvois, L. Duffours, ToF-SIMS depth profiling of altered glass, Npj Mater. Degrad. 3 (2019) 14. https://doi.org/10.1038/s41529-019-0076-3.
[48] F. Bouyer, G. Geneste, S. Ispas, W. Kob, P. Ganster, Water solubility in calcium aluminosilicate glasses investigated by first principles techniques, J. Solid State Chem. 183 (2010) 2786–2796. https://doi.org/10.1016/j.jssc.2010.08.031.
[49] P. Frugier, C. Martin, I. Ribet, T. Advocat, S. Gin, The effect of composition on the leaching of three nuclear waste glasses: R7T7, AVM and VRZ, J. Nucl. Mater. 346 (2005) 194–207. https://doi.org/10.1016/j.jnucmat.2005.06.023.
[50] C. Weigel, G. Calas, L. Cormier, L. Galoisy, G.S. Henderson, High-resolution Al $L_{2,3}$ -edge x-ray absorption near edge structure spectra of Al-containing crystals and glasses: coordination number and bonding information from edge components, J. Phys. Condens. Matter. 20 (2008) 135219. https://doi.org/10.1088/0953-8984/20/13/135219.
[51] M. Fournier, A. Ull, E. Nicoleau, Y. Inagaki, M. Odorico, P. Frugier, S. Gin, Glass dissolution rate measurement and calculation revisited, J. Nucl. Mater. 476 (2016) 140–154. https://doi.org/10.1016/j.jnucmat.2016.04.028.
[52] S. Gin, X. Guo, J.-M. Delaye, F. Angeli, K. Damodaran, V. Testud, J. Du, S. Kerisit, S.H. Kim, Insights into the mechanisms controlling the residual corrosion rate of borosilicate glasses, Npj Mater. Degrad. 4 (2020) 41. https://doi.org/10.1038/s41529-020-00145-2.
[53] G.N. Greaves, S. Sen, Inorganic glasses, glass-forming liquids and amorphizing solids, Adv. Phys. 56 (2007) 1–166. https://doi.org/10.1080/00018730601147426.
[54] R.J. Hand, D.R. Tadjiev, Mechanical properties of silicate glasses as a function of composition, J. Non-Cryst. Solids. 356 (2010) 2417–2423. https://doi.org/10.1016/j.jnoncrysol.2010.05.007.
[55] T. Charpentier, K. Okhotnikov, A.N. Novikov, L. Hennet, H.E. Fischer, D.R. Neuville, P. Florian, Structure of Strontium Aluminosilicate Glasses from Molecular Dynamics Simulation, Neutron Diffraction, and Nuclear Magnetic Resonance Studies, J. Phys. Chem. B. 122 (2018) 9567–9583. https://doi.org/10.1021/acs.jpcb.8b05721.
[56] R. Dupuis, J.S. Dolado, J. Surga, A. Ayuela, Doping as a Way To Protect Silicate Chains in Calcium Silicate Hydrates, ACS Sustain. Chem. Eng. 6 (2018) 15015–15021. https://doi.org/10.1021/acssuschemeng.8b03488.
[57] A. Pelmenschikov, H. Strandh, L.G.M. Pettersson, J. Leszczynski, Lattice Resistance to Hydrolysis of Si-O-Si Bonds of Silicate Minerals: Ab Initio Calculations of a Single Water Attack onto the (001) and (111) β-Cristobalite Surfaces, J. Phys. Chem. B. 104 (2000) 5779–5783. https://doi.org/10.1021/jp994097r.
[58] Y. Yu, B. Wang, M. Wang, G. Sant, M. Bauchy, Revisiting silica with ReaxFF: Towards improved predictions of glass structure and properties via reactive molecular dynamics, J. Non-Cryst. Solids. 443 (2016) 148–154. https://doi.org/10.1016/j.jnoncrysol.2016.03.026.
[59] R. Dupuis, R. Pellenq, J.-B. Champenois, A. Poulesquen, Dissociation Mechanisms of Dissolved Alkali Silicates in Sodium Hydroxide, J. Phys. Chem. C. 124 (2020) 8288–8294. https://doi.org/10.1021/acs.jpcc.0c01495.
[60] R. Dupuis, L.K. Béland, R.J.-M. Pellenq, Molecular simulation of silica gels: Formation, dilution, and drying, Phys. Rev. Mater. 3 (2019) 075603. https://doi.org/10.1103/PhysRevMaterials.3.075603.
[61] T.S. Mahadevan, W. Sun, J. Du, Development of Water Reactive Potentials for Sodium Silicate Glasses, J. Phys. Chem. B. 123 (2019) 4452–4461. https://doi.org/10.1021/acs.jpcb.9b02216.
[62] T.S. Mahadevan, S.H. Garofalini, Dissociative Chemisorption of Water onto Silica Surfaces and Formation of Hydronium Ions, J. Phys. Chem. C. 112 (2008) 1507–1515. https://doi.org/10.1021/jp076936c.

[63] B. Guillot, Y. Guissani, How to build a better pair potential for water, J. Chem. Phys. 114 (2001) 6720–6733. https://doi.org/10.1063/1.1356002.
[64] T.S. Mahadevan, J. Du, Evaluating Water Reactivity at Silica Surfaces Using Reactive Potentials, J. Phys. Chem. C. 122 (2018) 9875–9885. https://doi.org/10.1021/acs.jpcc.7b12653.
[65] H. Liu, Z. Fu, K. Yang, X. Xu, M. Bauchy, Machine learning for glass science and engineering: A review, J. Non-Cryst. Solids. 557 (2021) 119419. https://doi.org/10.1016/j.jnoncrysol.2019.04.039.
[66] M.A. Kraus, M. Drass, Artificial intelligence for structural glass engineering applications — overview, case studies and future potentials, Glass Struct. Eng. 5 (2020) 247–285. https://doi.org/10.1007/s40940-020-00132-8.
[67] R.K. Vasudevan, K. Choudhary, A. Mehta, R. Smith, G. Kusne, F. Tavazza, L. Vlcek, M. Ziatdinov, S.V. Kalinin, J. Hattrick-Simpers, Materials science in the artificial intelligence age: high-throughput library generation, machine learning, and a pathway from correlations to the underpinning physics, MRS Commun. 9 (2019) 821–838. https://doi.org/10.1557/mrc.2019.95.
[68] N.M. Anoop Krishnan, S. Mangalathu, M.M. Smedskjaer, A. Tandia, H. Burton, M. Bauchy, Predicting the dissolution kinetics of silicate glasses using machine learning, J. Non-Cryst. Solids. 487 (2018) 37–45. https://doi.org/10.1016/j.jnoncrysol.2018.02.023.
[69] H. Liu, T. Zhang, N.M. Anoop Krishnan, M.M. Smedskjaer, J.V. Ryan, S. Gin, M. Bauchy, Predicting the dissolution kinetics of silicate glasses by topology-informed machine learning, Npj Mater. Degrad. 3 (2019) 32. https://doi.org/10.1038/s41529-019-0094-1.

8 Appendices

Table A1: Statistical tests for the distribution of activation energies for bond dissociation of Si in pure silicate, Si and Al in aluminosilicate glass.

Atom type in glass	Type of test	P-Value	Type of distribution	Type of T-test selected	P-Values
Si in pure silicate	Kolmogorov-Smirnov test	0.00	Not normal distribution	Reference	Reference
Si in aluminosilicate	Kolmogorov-Smirnov test	0.00	Not normal distribution	Mann-whitney test	0.001
Al in aluminosilicate	Kolmogorov-Smirnov test	0.00	Not normal distribution	Mann-whitney test	0.00

Table A2: Statistical tests for the distribution of activation energies for dissociating Si in pure silicate glass based on the number of bridging oxygen atoms.

Type of coordination	Type of test	P-Value	Type of distribution	Type of T-test selected	P-Values
Si_4 --> Si_3	Kolmogorov-Smirnov test	0.00	Not normally distributed	Reference	Reference
Si_3 --> Si_2	Kolmogorov-Smirnov test	0.00	Not normally distributed	Mann-whitney test	0.034
Si_2 --> Si_1	Shapiro-Wilk test	0.696	Normally distributed	Mann-whitney test	0.102

Table A3: Statistical tests for the distribution of activation energies for dissociating Si in aluminosilicate glass based on the number of bridging oxygen atoms.

Type of coordination	Type of test	P-Value	Type of distribution	Type of T-test selected	P-Values
Si_4 --> Si_3	Kolmogorov-Smirnov test	0.00	Not normally distributed	Reference	Reference
Si_3 --> Si_2	Kolmogorov-Smirnov test	0.00	Not normally distributed	Mann-whitney test	0.393
Si_2 --> Si_1	Shapiro-Wilk test	0.1643	Normally distributed	Mann-whitney test	0.288

Table A4: Statistical tests for the distribution of activation energies for dissociating Al in aluminosilicate glass based on the number of bridging oxygen atoms.

Type of coordination	Type of test	P-Value	Type of distribution	Type of T-test selected	P-Values
Al_4-->Al_3	Shapiro-Wilk test	0.107	Normally distributed	Reference	Reference
Al_3-->Al_2	Shapiro-Wilk test	0.516	Normally distributed	Welch's t-test	0.882
Al_2-->Al_1	Shapiro-Wilk test	0.748	Normally distributed	Welch's t-test	0.541

Table A5: Statistical tests for the distribution of activation energies for dissociating Si in aluminosilicate glass based on the position of Al as the second neighbour.

Type of coordination	Type of test	P-Value	Type of distribution	Type of T-test selected	P-Values
Al_0	Kolmogorov-Smirnov test	0.00	Not normally distributed	Reference	Reference
Al_1	Kolmogorov-Smirnov test	0.00	Not normally distributed	Mann-whitney test	0.03
Al_2	Shapiro-Wilk test	0.21	Normally distributed	Mann-whitney test	0.006
Al_3	Shapiro-Wilk test	0.811	Normally distributed	Mann-whitney test	0.016
Al_4	Shapiro-Wilk test	0.003	Not normally distributed	Mann-whitney test	0.027

Table A6: Statistical tests for the distribution of activation energies for dissociating Al in aluminosilicate glass based on the position of Si as the second neighbour.

Type of coordination	Type of test	P-Value	Type of distribution	Type of T-test selected	P-Values
Si_4	Shapiro-Wilk test	0.304	Normally distributed	Reference	Reference
Si_3	Shapiro-Wilk test	0.508	Normally distributed	Welch's t-test	0.422
Si_2	Shapiro-Wilk test	0.97	Normally distributed	Welch's t-test	0.859

Table A7: Statistical tests for the correlation of bond angle, shear stress and hydrostatic pressure with activation energy for Si in pure silicate, Si and Al in aluminosilicate glass.

Atom in Glass type	P-values for bond angle vs activation energy	P-values for shear stress vs activation energy	P-values for hydrostatic pressure vs activation energy
Si in pure silicate	0.00	0.00	0.991
Si in aluminosilicate	0.028	0.0029	0.130
Al in aluminosilicate	0.02	0.9787	0.955

Fig. A. 1:

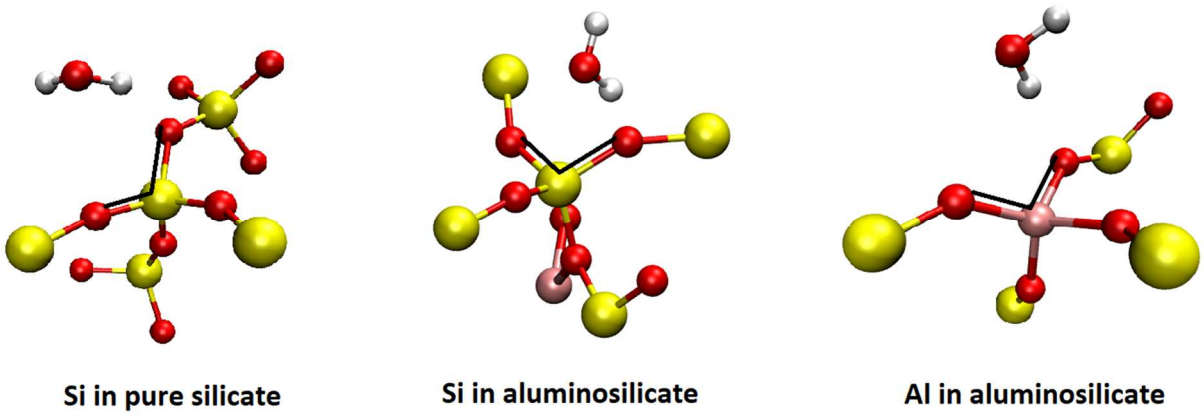

Fig. A. 1: Mechanism of dissociation of Si in pure silicate and Si, Al in aluminosilicate glass by water. O-Si-O and O-Al-O angles are widely open for providing way for the water molecule to interact and dissociate the bridge.

Mystery

Conc of Al in Silicate glass	Durability against water
No Al%	Moderate
Small Al%	High
More Al%	Very low

Method

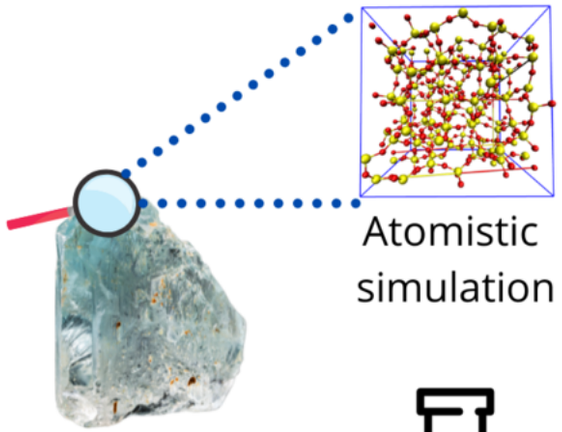

Results

Activation Energy (Ea) for bond dissociation

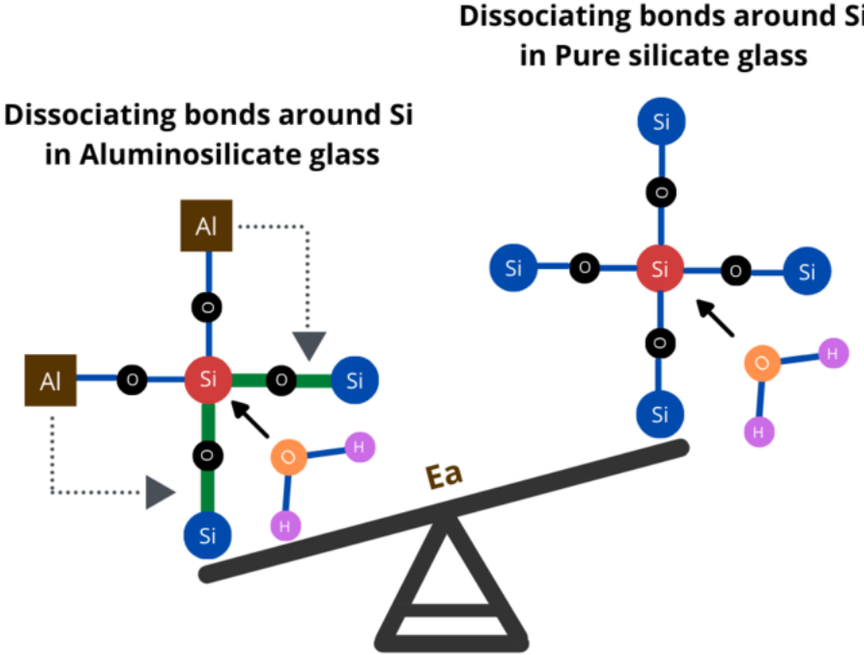

Conclusion: 1. Al is very easy to dissociate. 2. Al has ability to strengthen Si, so at small %, it increases durability against water. 3. Al at high %, preferential release of Al weakens the Si network, very low durability against water.